Totally Parameter Independent Speed Estimation of Synchronous Machines Based on Online Short Time Fourier Transform Ridges

G. El-Murr, D. Giaouris, and J.W. Finch

Abstract—High frequency signal injection is considered a parameter independent sensorless speed and position estimation technique which operates efficiently at low and zero speed. That is due to the saliency presence in the machine, which gives information about the rotor speed and position. Therefore the high frequency signal injected into the motor is modulated by the rotor speed and position information. Conventionally, to extract the useful information from the spectrum of the resultant signal, Phase-Locked Loop structure based demodulation schemes have been used. However, the PLL dynamics can be affected by the variation of inductances, PI parameters, and filter characteristics. In addition the error between the actual and estimated angle has to be small at the beginning of the estimation process. These restrictions are essential to maintain stability and to track the rotor speed and position accurately. However, such conditions are not always satisfied and are dependent on the operating conditions of the machine. Recently the concept of instantaneous frequency has become useful in many engineering applications where it is used to describe time varying signals. In this paper an instantaneous frequency estimation scheme based on the short time Fourier Transform ridges algorithm is proposed to detect the rotor speed and position. Theoretical and simulation aspects of the conventional and proposed methods are discussed and the obtained results are compared.

Index Terms— **Instantaneous frequency estimation, sensorless control.**

NOMENCLATURE

u_c, i_c	High frequency voltage and current vectors in stationary reference frame
u'_c, i'_c	High frequency voltage and current vectors transferred to the rotor reference frame
U_c	High frequency voltage amplitude
ω_c	Carrier frequency
ω_r	Rotor velocity
$dq, \alpha\beta$	Subscripts denoting rotor and stator direct and quadrature axes.
l	Leakage inductance
$\wedge$	Denotes estimated quantities
LPF	Lowpass filter

I. INTRODUCTION

Numerous sensorless techniques have been developed over past decades, their purpose being to accurately control the AC drives without mechanical position or speed sensor. There are two main categories of estimation methods: those which rely on the back-EMF voltage associated with fundamental component excitation of the machine (parameter dependent models) [1, 2], and those which use a second excitation signal in addition to the fundamental excitation (high frequency injection) [1-7].

The main drawback in most of the parameter dependant sensorless techniques is their inability to work at low and zero speed. Only high frequency signal injection methods operate efficiently at very low and zero speed [8, 9]. This is because in such schemes, the stator resistance as well as the back-EMF disturbance can be neglected, and the rotor speed and position estimation is only based on the inductance difference between the d-axis and q-axis (with reference to the synchronously rotating reference frame). Such an inductance difference may arise due to the physical rotor design differences between the d-axis and q-axis, e.g. with the use of flux barriers and/or Permanent Magnets (PM). However, operating conditions (working point) may have a large effect on the inductance difference, since saturation in general causes a decrease in inductance. Also, the stator winding design (e.g. using concentrated windings) and other phenomena like mutual and cross coupling may influence the inductance difference. Machines may be deliberately designed to exhibit the inductance difference, however in many cases it is inherently present. Such machines may include some PM Synchronous Machines (PMSM), interior-PMSM and even surface-mounted-PMSM, also some Reluctance Synchronous Machines (RSM) and PM-assisted-RSM.

In general, the injected high frequency, or carrier signal, is superimposed to the fundamental excitation. The carrier signal can be a balanced three-phase, voltage or current, applied in the

stator reference frame [10], or single phase sinusoidal signal applied in an arbitrary reference frame [11]. However high frequency voltage injection is preferable for these reasons: no additional voltage sensors are added to the sensorless drive, the limitations of the current fed inverter, high voltage sensor cost compared with current sensors which are much cheaper, also the resultant current can be measured using the current sensors already in the sensorless control drive [2].

The resultant high frequency current is amplitude modulated by the error between the actual and the estimated rotor position. To extract the useful information, observers based on the Phase Locked Loop (PLL) structure are used. However, some restrictions are required for the PLL observer to maintain stability and produce accurate results. These are: the error between the estimated and actual rotor angle should be small, and the input carrier frequency should be synchronized with the demodulator carrier frequency. In addition to the restrictions stated previously, the PLL response can be affected by the variation of d-q inductances [12-14]. As a result the PLL parameters must be tuned depending on the characteristics of the machine and the operating state.

Recently the application of advanced signal processing techniques in electric drives [15, 16] have improved the performance of such systems, and with the help of advanced DSP technology more sophisticated signal processing methods can be applied.

In this paper, a new demodulation technique is proposed. It is applicable for the rotating voltage injection method and the rotor speed can be determined using online Short Time Fourier Transform (STFT) Ridges. The proposed method is completely parameter independent and it is even more efficient than the PLL under any condition. Such technique can be implemented on DSP's to perform the calculation of the Fourier transformation and ridges algorithm. Theoretical analysis for the conventional and proposed methods are analysed and the results are presented in section V.

II. HIGH FREQUENCY VOLTAGE INJECTION

The interaction of the machine saliency with the injected high frequency voltage produces a high frequency current modulated by the rotor position and speed information. Fig.1 illustrates the general idea of the high frequency injection method.

In the cageless interior-PMSM the saliency exists due to the asymmetric structure of the motor and the d-q inductance difference is usually large. However for the surface mounted PMSM the magnetic anisotropy is induced by the saturation of the main flux [17]. The anisotropy is defined to be the d-q inductance difference induced by the magnetic flux saturation.

To reduce the effect of parameter dependency of the estimator especially at zero and very low speed, a balanced 3-phase high frequency voltage (1) can be injected into the machine, Table. I.

$$\boldsymbol{u}_c = \begin{bmatrix} u_{c\alpha} \\ u_{c\beta} \end{bmatrix} = U_\varepsilon \begin{bmatrix} \cos\left(\omega_c t\right) \\ \sin\left(\omega_c t\right) \end{bmatrix} \tag{1}$$
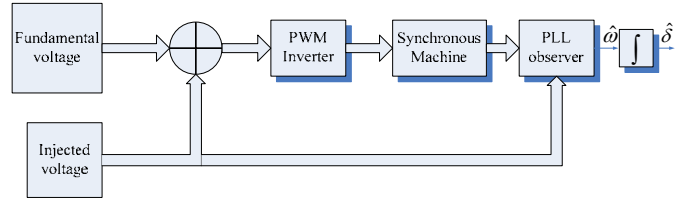

Fig.1: Block diagram of the conventional high frequency injection scheme

The carrier frequency range can vary between 600Hz and 2 kHz depending on the machine characteristics, and the sampling frequency of the inverter.

At high frequency, the motor model can be expressed as a purely inductive load:

$$\boldsymbol{u}'_c = l\frac{d\boldsymbol{i}'_c}{dt} \tag{2}$$

The voltage injection results in a high frequency current superimposed to the fundamental excitation. The high frequency component can be extracted using a bandpass filter centered at the carrier frequency. Thus the resultant high frequency current (3) is modulated by the rotor frequency.

$$\boldsymbol{i}'_c = -j\frac{U_c}{(\omega_c - \omega_r)} \begin{bmatrix} \dfrac{\cos\left((\omega_c - \omega_r)t\right)}{l_d} \\ \dfrac{\sin\left((\omega_c - \omega_r)t\right)}{l_q} \end{bmatrix} \tag{3}$$

The transformation of (3) to the stationary reference frame yields:

$$\boldsymbol{i}_c = \begin{bmatrix} i_{c\alpha} \\ i_{c\beta} \end{bmatrix} = K \begin{bmatrix} (l_d + l_q)\sin(\omega_c t) - (l_d - l_q)\sin\left(\omega_c t - 2\omega_r t\right) \\ (l_d + l_q)\cos(\omega_c t) + (l_d - l_q)\cos\left(\omega_c t - 2\omega_r t\right) \end{bmatrix} \tag{4}$$

where $K = \dfrac{U_c}{\omega_c - \omega_r}$

The high frequency current signal contains positive and negative sequence components. Only the negative sequence current component contains the desired information related to the rotor position.

To extract the information from the negative sequence current component, the resultant high frequency current (4) is transformed to another reference frame rotating at an angular velocity $\omega_c - 2\hat{\omega}_r$. The obtained equation can be represented using Euler formula as:

$$\boldsymbol{i}_c^{\omega_c - 2\hat{\omega}_r} = -j\frac{u_c}{2(\omega_c - \omega_r)l_d l_q} \left(\begin{array}{c} (l_d + l_q)e^{j(2\omega_c t - 2\hat{\omega}_r t)} \\ + (l_q - l_d)e^{j(2\omega_r t - 2\hat{\omega}_r t)} \end{array} \right) \tag{5}$$

By lowpass filtering and extracting the real part of equation (5), the resultant low frequency signal can be written as:

$$LPF(\boldsymbol{i}_c^{\omega_c - 2\hat{\omega}_r}) = \frac{u_c}{(\omega_c - \omega_r)l_d l_q}\sin\delta \tag{7}$$

For a small position difference:

$$\sin\delta = \Delta\delta \tag{8}$$

where $\Delta\delta = \delta_r - \hat{\delta}_r$ is the error between the actual and estimated rotor position.

To find the rotor position a closed loop control system based

on the PLL strategy has been used. The PLL consists of a demodulator, PI controller, and an integrator.

Table. I
Motor Parameters

Symbol	Quantity	Value (unit)
V_{rated}	Rated voltage	400/460 (v)
P	Pole pair	2
R_s	Stator resistance	6.25 (Ω)
l_d	Stator d-axis inductance	142 (mH)
l_q	Stator q-axis inductance	380 (mH)
ω_{rated}	Rated speed	6000 (rpm)

III. PROPOSED DEMODULATION SCHEME

It has been mentioned in section II that the PLL based observer is unable to lock unless the error between the actual and estimated angle is small. For this approximation the PI parameters should be set to prevent the nonlinearity of the resultant error (7) produced after low-passing the multiplication of the incoming and the reference signal. However, a sophisticated PLL can be designed to compensate for the nonlinearity problem but this will lead to a latency in the output response and increase in the cost. On the other hand an additional higher order filter can be added to the drive to solve the noise interference. These filters can affect the performance and stability of the system.

To remove the effect of amplitude variation, caused by the inductance variation, of the current signal on the tracking process, a new demodulation technique is proposed. The quadrature and direct high frequency stator current components can be multiplied by each other to produce another vector represented as follows:

$$i_{c\alpha} \times i_{c\beta} = K_1^2 \sin(\omega_c t) - K_1 K_2 \sin(2\omega_c t + 2\omega_r t) + K_1 K_2 \sin(2\omega_r t) + K_2^2 \sin(2\omega_c t + 4\omega_r t) \tag{9}$$

$$LPF(i_{c\alpha} \times i_{c\beta}) = K_1 K_2 \sin(2\omega_r t) \tag{10}$$

where, $K_1 = \dfrac{U_c}{2\omega_c l_d l_q}(l_d + l_q)$ and $K_2 = \dfrac{U_c}{2\omega_c l_d l_q}(l_q - l_d)$

Also, $i_{c\alpha}$ and $i_{c\beta}$ are delayed by $\dfrac{\pi}{4}$, multiplied by each other and then filtered:

$$(i_{c\alpha} \times i_{c\beta})_{delayed} = K_1^2 \cos(\omega_c t) - K_1 K_2 \cos(2\omega_c t + 2\omega_r t) + K_1 K_2 \cos(2\omega_r t) + K_2^2 \cos(2\omega_c t + 4\omega_r t) \tag{11}$$

$$LPF(i_{c\alpha} \times i_{c\beta})_{delayed} = K_1 K_2 \cos(2\omega_r t) \tag{12}$$

Using equations (10)(12) the speed and rotor position can be determined by applying advanced Instantaneous Frequency (IF)estimation algorithms such as zero-crossing, adaptive IF filters, Time-Frequency distribution etc.

However, equations (10) and (12) cannot be used directly to estimate instantaneously the rotor speed and consequently the position. Thus a frequency shift signal processing scheme described in equation (13) is proposed.

The frequency shift method enables a decrease in the time period, which contains the information related to the rotor speed, in comparison to the period of the signals in (10) or (12). Therefore the estimator will be able to detect the instantaneous rotor speed and position in transient and steady state conditions As a result the proposed estimation scheme is able to provide useful information for sensorless control.

$$i_h = K_1 K_2 \left(\sin(2\omega_r t) \times \cos(\omega_h t) + \cos(2\omega_c t) \times \sin(\omega_h t)\right)$$
$$= K_1 K_2 \sin(\omega_h + 2\omega_r)t \tag{13}$$

where i_h is the resultant shifted signal, and ω_h is the frequency by which the actual rotor frequency is shifted

IV. ONLINE STFT RIDGES METHOD USED TO ESTIMATE THE INSTANTANEOUS ROTOR SPEED

The Fourier Transform (FT) plays a fundamental role in the analysis of signals and time invariant linear systems. The efficiency of the FT is that it describes the relation between a signal in time domain and frequency domain (14).

$$X(f) = \int_{-\infty}^{+\infty} x(t)e^{-j2\pi ft} dt \tag{14}$$

where $X(f)$ is the Fourier transform of $x(t)$, and f is the variable frequency. As shown in (14) the analysis coefficient of $X(f)$ are computed as inner products of the signal with sine-wave functions of infinite duration. A result of the infinite extent of the FT analysis is that the results are time averaged. Thus it contains only globally averaged information and so hides transients or locations of specific features within the signal. Consequently any abrupt change in time in a non-stationary (time varying) signal $x(t)$ is spread out over the whole frequency.

This limitation can be partly overcome by introducing a sliding time window of fixed length to localize the analysis in time. This concept is called Short Time Fourier Transform (STFT), and is defined as:

$$S(\tau, f) = \int_{-\infty}^{+\infty} x(t)g(t-\tau)e^{-j2\pi ft} dt \tag{15}$$

where $g(t-\tau)$ is the sliding window function

For instantaneous time-frequency representation of the signal the spectrogram is commonly used in to investigate the time frequency content of the signal. The spectrogram $P_s(\tau,f)$ is nothing more the STFT squared:

$$P_s(\tau, f) = \left| \int_{-\infty}^{+\infty} x(t)g(t-\tau)e^{-j2\pi ft} dt \right|^2 \tag{16}$$

The energy spectral density $E(f)$ describes how the energy of a (finite-energy) signal is distributed with frequency (17)

$$E(f) = \left| \frac{1}{\sqrt{2\pi}} \int_{-\infty}^{+\infty} x(t)e^{-j2\pi ft} dt \right|^2 \tag{17}$$

The difference between equation (17) and (16) is the time localisation of the window function $g(t)$. As a result the spectrogram representation can be defined as the distributed
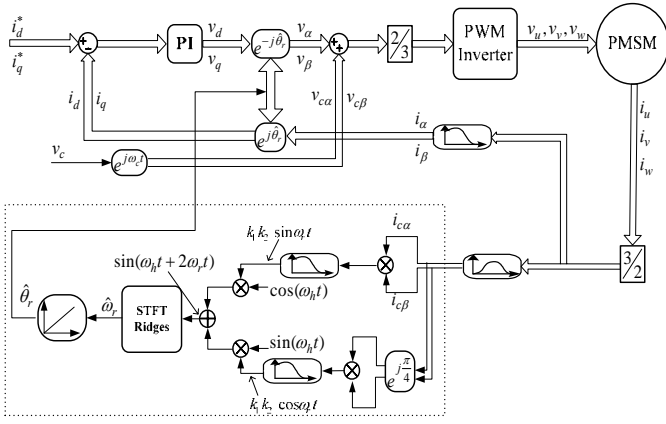
Fig.2: Sensorless control block diagram using STFT Ridges algorithm

energy of a signal localised in the time boundary of the translated window function.

According to [18] the energy density of a signal is mainly concentrated around the instantaneous frequency, which means that the maximum time-frequency energy distribution is located around the instantaneous frequency. Thus the frequency can be estimated by extracting the peak value of the spectrogram and its associated frequency. This can be done by using the ridges algorithm described in [18, 19] .

In sensorless control of PMSM the rotor speed must be estimated instantaneously integrated and fed-back to the controller Fig.2. Therefore the STFT ridges estimator should estimate the rotor speed online. In real time applications the spectrogram of a signal can be found efficiently by using discrete-time STFT:

$$P_s(m,f) = \left| \sum_{n=-\infty}^{+\infty} i_h(n)g(n-m)e^{-j2\pi fn} \right|^2 \qquad (17)$$

The time window of the spectrogram can be minimised by using equation (13). Thus the instantaneous frequency of the signal i_h can be estimated rapidly by finding the maximum value of the spectrum during the (time window =0.001s).

V. DISCUSSION AND RESULTS

The conventional PLL method often used to estimate the rotor speed has been discussed. A frequency estimation technique based on STFT Ridges has been suggested to improve the performance of the high frequency injection scheme.

To verify the performance of the proposed method, PMSM and the estimator have been modeled using Matlab, and the PMSM parameters used are shown in Table 1. The band-pass filters used are Butterworth second order filters centered at 1.5 kHz with 400 Hz bandwidth, and the FFT length used in the STFT ridges estimator is 2^{16}.The amplitude of the injected voltage is 15V and the carrier frequency is 1.5 kHz.

During the tests the voltage is applied directly to the machine without any control scheme. Therefore the rotor speed is oscillating during the transient state due to the lack of

synchronisation between the rotor flux and the stator flux in the
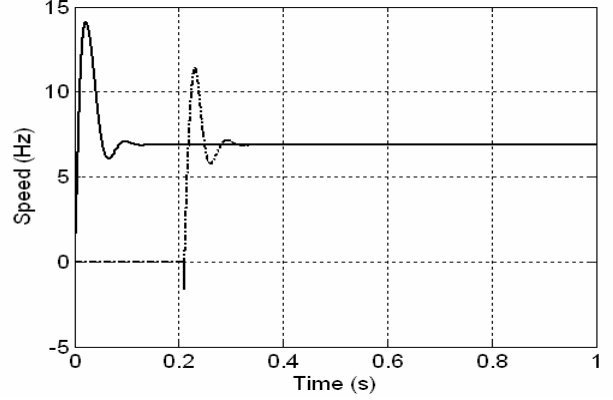
a) Actual rotor speed (solid line), PLL estimated speed (dashed line)
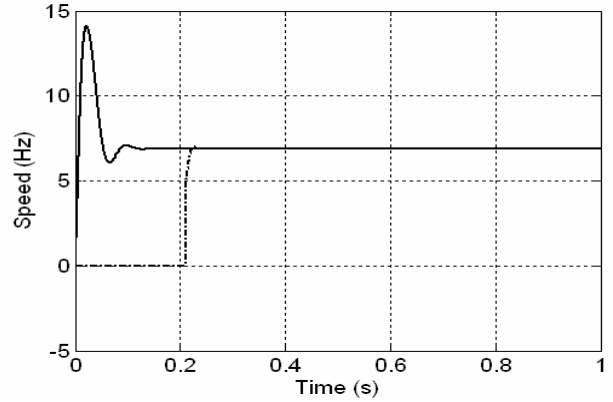
b) Actual rotor speed (solid line), STFT estimated speed (dashed line)

Fig.3: Motor running at a speed equal to 6.9 Hz

start-up region. Such tests can be performed at low speed since the rotor flux will be able to lock on the stator flux after some delay, otherwise the machine may slip and the rotor never turn.

The estimator response of the PLL is presented in Fig. 3; the estimator is turned on after the machine reaches the steady state region. It can be seen clearly that a large overshoot occurs in the response. This is due to the damping ratio of the filters, the parameters of the PI controller, and the amplitude of the resultant current signal. However in Fig. 4 the overshoot disappeared and the STFT ridges estimator reaches the steady state region even faster then the PLL observer. This can be explained as: the STFT ridges estimator is dependant only on the frequency of the signal and it is completely independent from any current amplitude variations or filter parameters. In addition the rapidity of the response can be easily tuned by the high frequency signal (13) and the time window.

Moreover the PLL response is dependant on the difference between the actual and the estimated rotor angle (8). This can be proved by comparing the PLL response at different rotor speed and in the reverse speed direction. The machine is subjected to a sudden reverse speed command. The PLL detected the speed faster at low speed, whereas for the high speed the PLL takes time to lock. On the other hand, the results obtained using STFT method show that the response of the proposed estimator remains the same under any speed
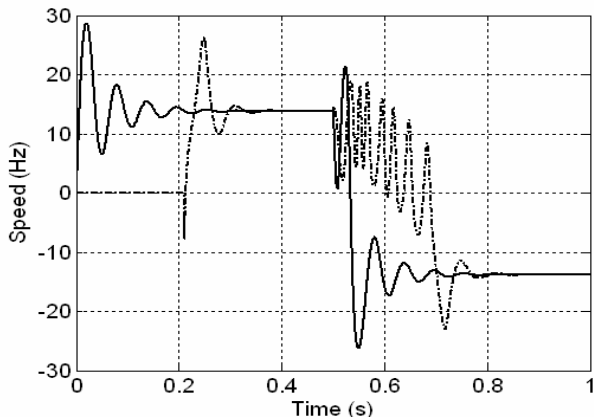
command.
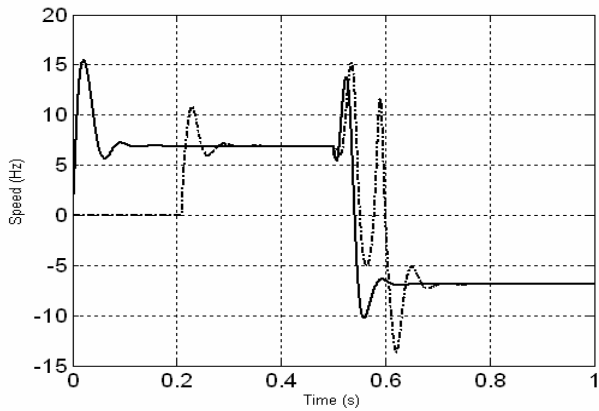
a) Actual rotor speed (solid line), PLL estimated speed (dashed line)
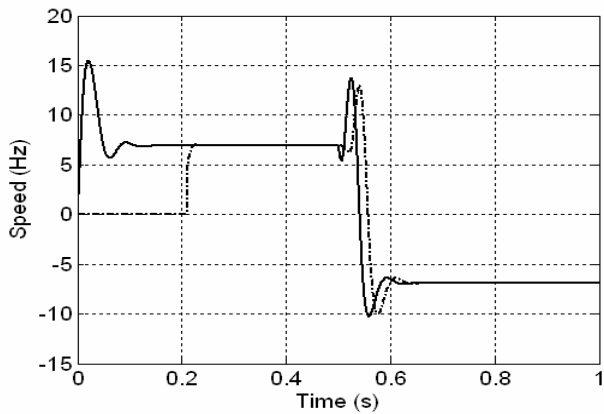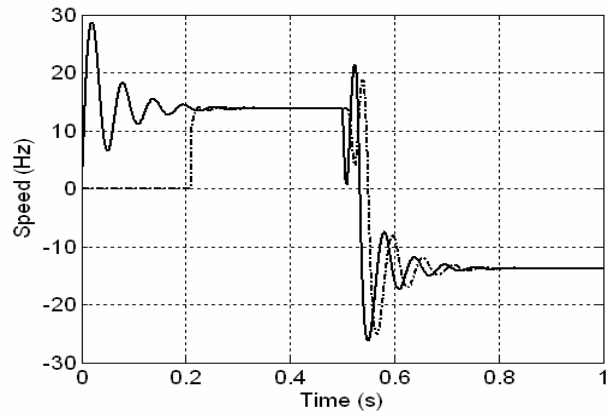

b) Actual rotor speed (solid line), STFT estimated speed (dashed line)

Fig.4: the machine is operating at forward (6.9Hz) and reverse speed (-6.8Hz)

b) Actual rotor speed (solid line), STFT estimated speed (dashed line)

Fig.5: -a) The effects of large angle error (8),on the response of the PLL shown clearly when the machine is operating at 13.4 Hz, and is then subjected to a sudden reverse speed -13.4 Hz. b) The STFT estimator response is not affected.

a) Actual rotor speed (solid line), PLL estimated speed (dashed line)

b) Actual rotor speed (solid line), STFT estimated speed (dashed line)

Fig.6: Load has been applied to the machine; transient speed variation has been occurred before the speed returns to the steady state value 6.9Hz.

In the results showing in Fig. 6 both estimators have been tested during transient and steady state motor operation. The motor is subjected to a load in order to create a transient state on the rotor speed. A small variation has been occurred, due to the impact of the load, before the speed returns to the steady state value (6.5Hz). Opposite to the PLL observer, the STFT ridges estimator is capable in detecting the transient speed variation but with some delay due to the processing time.
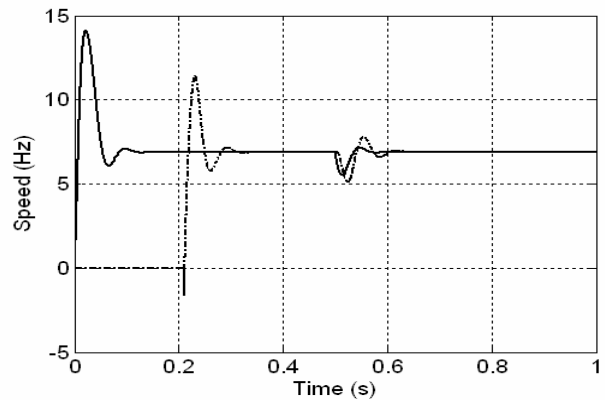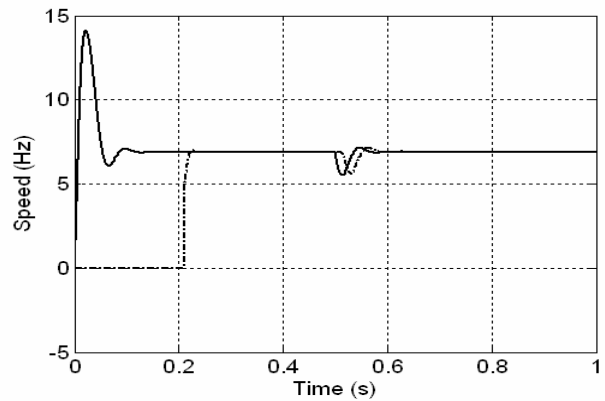
Finally the speed estimators have been tested at zero speed, Fig.7. The rotor speed has been tracked accurately by the conventional and the proposed estimation technique.
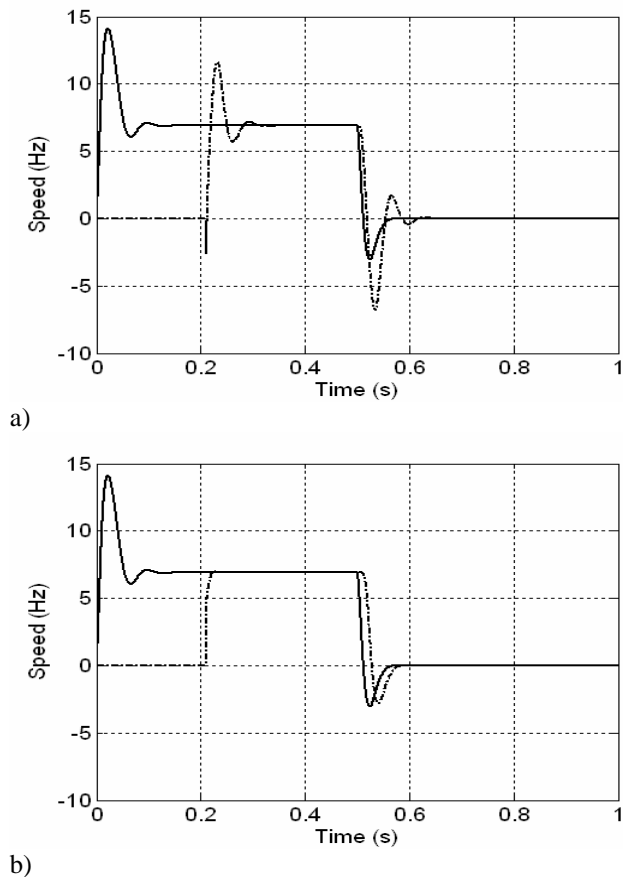

a) Actual rotor speed (solid line), PLL estimated speed (dashed line)

Fig.7: Motor first operating at 6.9 Hz then at 0 Hz (solid line): a) the PLL estimate (dashed line) b) the STFT ridges estimated speed (dashed line

VI. CONCLUSION

The main objective of the paper is to replace the PLL, which is affected by the inductance variations, by another totally parameter independent speed estimation method. The proposed scheme can be split into two parts; first the demodulation and then estimation part. The new method has been tested on the PMSM but it can be applied to another synchronous machine. Also, it has been shown better performance than the conventional PLL but it requires additional computational power. However, with the advanced microcontroller and DSP technologies this problem can be solved. In some applications the difference in d-q inductance can vary and becomes relatively small. Thus the SNR decreases and the PLL may loose track unless it is adjusted and higher order filters are added. The STFT ridges method used has additional advantage over the PLL is that it can operate at low SNR without any additional devices or parameter adjustments. Finally it is important to note that the proposed high frequency injection can detect the rotor frequency and by integrating the speed the rotor position can be found. Thus the initial position of the rotor should be known prior to the start of the estimation process

REFERENCES

[1] J. Holtz, "Sensorless Control of Induction Motors-Performance and Limitations," *Industrial Electronics. ISIE 2000. Proceedings of the 2000 IEEE International Symposium on*, vol. 1, pp. PL12-PL20, 2000.

[2] P. Vas, "Sensorless Vector and Direct Torque Control," *Oxford, U.K.: Oxford Univ.Press*, 1998.

[3] J. Ji-Hoon, S. Seung-Ki, H. Jung-Ik, K. Ide, and M. Sawamura, "Sensorless Drive of Surface-Mounted Permanent-Magnet Motor by High-Frequency Signal Injection Based on Magnetic Saliency," *IEEE Trans. on Industry Applications*, vol. 39, pp. 1031-1039, 2003.

[4] P. L. Jansen, M. Corley, and R. D. Lorenz, "Flux, Position, and Velocity Estimation in AC Machines at Zero and Low Speed Via Tracking of Frequency Saliency," *In Proc. EPE Conference*, pp. 154-160, 1995.

[5] M. J. Corley and R. D. Lorenz, "Rotor Position and Velocity Estimation for a Salient-Pole Permanent Magnet Synchronous Machine at Standstill and High Speeds," *IEEE Transactions on Industry Applications*, vol. 34, pp. 784-789, 1998.

[6] J. Yu-seok, R. D. Lorenz, T. M. Jahns, and S. Seung-Ki, "Initial Rotor Position Estimation of an Interior Permanent-Magnet Synchronous Machine Using Carrier Frequency Injection Methods," *IEEE Transactions on Industry Applications*, vol. 41, pp. 38-45, 2005.

[7] T. Noguchi, K. Yamada, S. Kondo, and I. Takahashi, "Initial Rotor Position Estimation Method of Sensorless PM Synchronous Motor with no Sensitivity to Armature Resistance," *IEEE Transactions on Industrial Electronics*, vol. 45, pp. 118-125, 1998.

[8] A. Consoli, G. Scarcella, and A. Testa, "Industry Application of Zero-Speed Sensorless Control Techniques for PM Synchronous Motors," *IEEE Transactions on Industry Applications*, vol. 37, pp. 513-521, 2001.

[9] T. Aihara, A. Toba, T. Yanase, A. Mashimo, and K. Endo, "Sensorless Torque Control of Salient-Pole Synchronous Motor at Zero-Speed Operation," *IEEE Transactions on Power Electronics*, vol. 14, pp. 202 - 208, 1999.

[10] P. L. Jansen and R. Lorenz , "Transducerless Position and Velocity Estimation in Induction and Salient AC Machines," *IEEE Transactions on Industrial Applications*, vol. 31, pp. 240-247, 1995.

[11] M. Linke, R. Kennel, and J. Holtz, "Sensorless Position Control of Permanent Magnet Synchronous Machines without Limitations at Zero Speed," *IEEE Annual Conference, Industrial Electronics Society*, vol. 1, pp. 674-679, 2002.

[12] Y. Li, Z. Q. Zhu, D. Howe, and C. M. Bingham, "Modeling of Cross-Coupling Magnetic Saturation in Signal-Injection-Based Sensorless Control of Permanent-Magnet Brushless AC Motors," *Magnetics, IEEE Transactions on*, vol. 43, pp. 2552-2554, 2007.

[13] P. Guglielmi, M. Pastorelli, and A. Vagati, "Cross-Saturation Effects in IPM Motors and Related Impact on Sensorless Control," *IEEE Transactions on Industry Applications*, vol. 42, pp. 1516-1522, 2006.

[14] J. Hu, L. Xu, and J. Liu, "Eddy Current Effects on Rotor Position Estimation for Sensorless Control of PM Synchronous Machine," *Industry Applications Conference, 2006. 41st IAS Annual Meeting. Conference Record of the 2006 IEEE*, vol. 4, pp. 2034-2039, 2006.

[15] D. Giaouris, J. W. Finch, O. C. Ferreira, R. Kennel, and G. El-Murr, "Wavelet Denoising for Electric Drives," *IEEE Transactions on Industrial Electronics*, to be published in 2008.

[16] J. M. Aller, T. G. Habetler, R. G. Harley, R. M. Tallam, and S. B. Lee;, "Sensorless Speed Measurement of AC Machines Using Analytic Wavelet Transform," *IEEE Transactions on Industry Applications*, vol. 38, pp. 1344-1350, 2002.

[17] J. Holtz and H. Pan, "Acquisition of Rotor Anisotropy Signals in Sensorless Position Control Systems," *IEEE Transactions on Industry Applications*, vol. 40, pp. 1379-1387, 2004.

[18] N. Delpart, B. Escudié, P. Guillemain, R. Kronland-Marinet, P. Tchamichian, and B. Torésani, "Asymptotic Wavelet and Gabor Analysis: Extraction of Instantaneous Frequencies," *IEEE Transactions on Information Theory*, vol. 38, pp. 644 - 664, 1992.

[19] R. A. Carmona, W. L. Hwang, and B. Torrésani, "Characterization of Signals by the Ridges and their Wavelet Transforms," *IEEE Transactions on Speech, and Signal Processing*, vol. 45, pp. 2586 - 2590, 1997.